

Galloping analysis of roof structures

Xiangting Zhang[†]

Department of Engineering Mechanics and Technology and Center for Civil Infrastructure Systems Research, Tongji University, Shanghai 200092, China

Ray Ruichong Zhang[‡]

Division of Engineering, Colorado School of Mines, Golden, Colorado 80401, USA

(Received June 23, 2002, Accepted January 24, 2003)

Abstract. This paper presents galloping analysis of multiple-degree-of-freedom (MDOF) structural roofs with multiple orientations. Instead of using drag and lift coefficients and/or their combined coefficient in traditional galloping analysis for slender structures, this study uses wind pressure coefficients for wind force representation on each and every different orientation roof, facilitating the galloping analysis of multiple-orientation roof structures. In the study, influences of nonlinear aerodynamic forces are considered. An energy-based equivalent technique, together with the modal analysis, is used to solve the nonlinear MDOF vibration equations. The critical wind speed for galloping of roof structures is derived, which is then applied to galloping analysis of roofs of a stadium and a high-rise building in China. With the aid of various experimental results obtained in pertinent research, this study also shows that consideration of nonlinear aerodynamic forces in galloping analysis generally increases the critical wind speed, thus enhancing aerodynamic stability of structures.

Key words: aerodynamic instability; galloping analysis; multiple-orientation roof structures; energy-based equivalent technique.

1. Introduction

Galloping or aerodynamic instability of civil structures is among the major concerns in wind-resistant structural design. In China, validation of structural capacity to resist aerodynamic instability is required for almost all the major design projects of large-scale structures (e.g., Shanghai Oriental-Pearl TV Tower in 1995, New Shanghai Stadium in 1997, and Shanghai Nanpu Great Bridge in 1998).

Historically, the pioneering work on galloping analysis dates back to Glauert and Hartog (Glauert 1919, and Hartog 1932 & 1956). Since then, significant developments have been made for in-depth understanding of galloping phenomena. Among them may be mentioned of experimental and theoretical work by Novak (1969, 1972), Kolousek *et al.* (1984), and Simiu and Cook (1992). Their studies focus, however, primarily on linear single-degree-of-freedom (SDOF) vibration analysis of a

[†] Director and Professor

[‡] Associate Professor

cross-section of slender prismatic structures using combined drag and lift coefficient for aerodynamic force representation. This restricts practical applications of the approach from a broad spectrum of structures such as roofs of stadium and building, of which no representative cross-section can be taken for galloping analysis.

This study extends the previous galloping analyses to the multiple-degree-of-freedom (MDOF) roof structures. Structural roofs are typically more vulnerable to the vertical wind responses than the horizontal wind responses. This study is, therefore, focused on the galloping analysis of roofs in the vertical direction. Instead of using the drag and lift coefficients and/or their combined coefficient in traditional galloping analysis, this study uses wind pressure shape coefficients for wind force representation on each and every different orientation roof, enabling the galloping analysis of multiple-orientation roof structures. The influences of nonlinear aerodynamic forces are examined in the study. An energy-based equivalent technique, together with the modal analysis, is adopted to solve the nonlinear MDOF vibration equations. In addition, various experimental results obtained in recent pertinent studies (Linder 1992, Okajima 1993, Kushioka *et al.* 1996, and Sohankar *et al.* 1997) are also used in the study for comprehensive understanding of galloping of MDOF structures in general and roofs in particular.

2. Governing equations for galloping of an MDOF system

Fig. 1 shows a multiple-degree-of-freedom (MDOF) structural system with multiple-orientation roofs subject to an incident wind flow with velocity v_r , while Fig. 2 illustrates the i -th sub-area of a

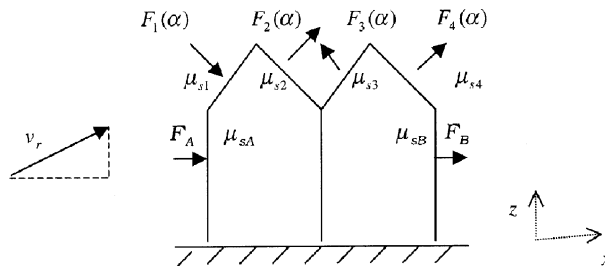


Fig. 1 Schematic diagram of a roof structure under wind loads

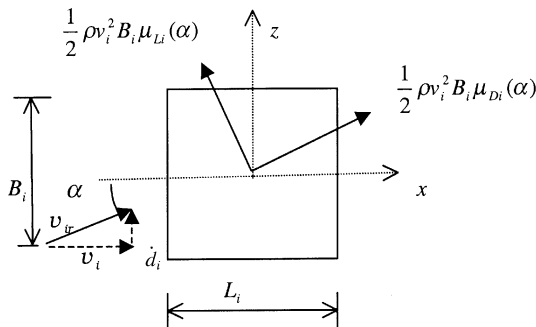


Fig. 2 Lift and drag forces on the i -th section of prismatic structure

roof under the wind flow. The wind flow has an attack angle α with the x -direction. Wind flow generates wind forces, which are normal to each and every structural plane such as F_j ($j=A, B$ and $1,2,3,4$) in Fig. 1. Therefore, the wind forces on structural vertical walls or columns (e.g., F_A and F_B in the x -direction in Fig. 1) do not attribute force components in the z -direction. The governing equations of the roofs in the z -direction are

$$[M]\{\ddot{d}\} + [C]\{\dot{d}\} + [K]\{d\} = \{F\} \quad (1)$$

where $[M]$, $[C]$ and $[K]$ are respectively the mass, damping and stiffness matrices of the structure, $\{d\}$ is the displacement vector in the z -direction, $\{F\}$ is the wind force vector and its i -th element can be found as

$$F_i = \frac{1}{2}\rho v_i^2 \sum_{k=1}^m A_k \mu_{sk}(\alpha) \cos \gamma_k \quad (2)$$

in which ρ is the mass density of air (t/m^3), v_i is the wind velocity at the i -th mass, m is the number of windward area, A_k is the k -th windward area, μ_{sk} is the wind pressure shape coefficient (the notation is generally used in China including Chinese Loading Code), γ_k is the angle between normal direction for the k -th area and the z -direction.

For prismatic structures with a regular cross-section (e.g., see Fig. 2), F_i in Eq. (2) can be alternatively expressed as

$$F_i = \frac{1}{2}\rho v_i^2 A_i \mu_{DLi}(\alpha), \quad A_i = B_i L_i \quad (3)$$

where B_i and L_i are respectively the windward cross-section width and length of the structure, $\mu_{DLi}(\alpha)$ is the combined coefficient for aerodynamic force representation that can be found in terms of drag coefficient $\mu_D(\alpha)$ and lift coefficient $\mu_L(\alpha)$ as follows

$$\mu_{DLi}(\alpha) = -[\mu_{Di}(\alpha)\tan(\alpha) + \mu_{Li}(\alpha)]\sec(\alpha) \quad (4)$$

It can be shown that Eq. (4) can also be represented in terms of the wind pressure shape coefficients.

However, since the attack angle changes as the orientation of each roof or i -th element varies, it is inconvenient using drag coefficient $\mu_D(\alpha)$ and lift coefficient $\mu_L(\alpha)$ (or their combined coefficient $\mu_{DL}(\alpha)$) to analyze the galloping of MDOF structures with irregular cross-sections such as roofs, in comparison with the use of the wind pressure shape coefficient μ_s . Accordingly, the traditional approach, i.e., galloping analysis of a regular cross-section of slender structures with the use of lift coefficient for wind lift force representation (see Simiu and Scanlan 1995), cannot simply and conveniently be extended to the problem under investigation.

Wind attack angle α is very small in comparison with unit. Therefore $\mu_s(\alpha)$ (or $\mu_{DL}(\alpha)$) can be expanded as a Taylor series as follows

$$\mu_s(\alpha) = \mu_s(0) + \mu'_s(0)\alpha + \frac{1}{2!}\mu''_s(0)\alpha^2 + \dots \quad (5a)$$

where the prime denotes the derivative of the function $\mu_s(\alpha)$ with respect to α . In addition, the following approximation is also valid for small α for the i -th element (Glauert 1919, Hartog 1932 & 1956, and Simiu and Cook 1992, etc.).

$$\alpha \approx \tan(\alpha_i) = \frac{\dot{d}_i}{v_i} \quad (5b)$$

where \dot{d}_i and v_i are the velocity components respectively in the z - and x -directions, as shown in Fig. 2.

With the use of modal analysis, the displacement vector has the following representation

$$d_i(t) = \sum_j \phi_{ij} q_j(t) \quad (6)$$

where $q_j(t)$ is the j -th generalized coordinate (or modal participation coefficient), and ϕ_{ij} is the i -th element of the j -th vibration mode $\phi_j(z)$. With the aid of Eqs. (4)-(6), Eq. (1) can be decoupled as the following equations

$$M_j^* \ddot{q}_j(t) + C_j^* \dot{q}_j(t) + K_j^* q_j(t) = F_j^*(\alpha) \quad (7)$$

where

$$\chi_j^* = \{\phi_j\}^T [\chi] \{\phi_j\} \quad ; \quad \chi = M, C, K \quad (8)$$

$$F_j^*(\alpha) = \sum_l C_{jFl}^* \cdot \frac{1}{v_0^{l-1}} (\dot{q}_j)^l = \sum_l \frac{1}{2} \rho v_0 \bar{C}_{jFl}^* \cdot \frac{1}{v_0^{l-1}} (\dot{q}_j)^l \quad (9)$$

$$\bar{C}_{jFl}^* = \{\phi_j\} [U^{(l)}(0)] \left\{ \left(\frac{\phi_j}{\sqrt{\mu_z}} \right)^l \right\} / l! \quad (10)$$

$$U_i^{(l)}(0) = \mu_z(z_i) \sum_{k=1}^m A_K \cos \gamma_k \frac{d^l \mu_{sk}(\alpha=0)}{d\alpha^l} \quad (11a)$$

or

$$U_i^{(l)}(0) = \mu_z(z_i) A_i^* \frac{d^l \mu_{DL}(\alpha=0)}{d\alpha^l}, \quad A_i^* = B_i L_i \quad (11b)$$

where use has been made of $\dot{d}_i = \sum_j \phi_{ij} \dot{q}_j(t)$ and $v_i = v_0 \sqrt{\mu_z(z)}$, in which v_0 is the basic wind speed at 10 m high, μ_z is the coefficient relating the wind pressures at heights 10 m and z_i .

When linear terms of α or \dot{q} are considered only in Eqs. (5)-(11), i.e., $l=0$ and 1 in Eqs. (9)-(11), Eq. (7) becomes

$$\begin{aligned}
M_j^* \ddot{q}_j(t) + (C_j^* - C_{jF1}^*) \dot{q}_j(t) + K_j^* q_j(t) &= F_j^*(0) \\
C_j^* &= \{\phi_j\}^T [C] \{\phi_j\} = 2 \zeta_j \omega_j M_j^* \\
C_{jF1}^* &= \frac{1}{2} \rho v_0 \cdot \bar{C}_{jF1}^* = \frac{1}{2} \rho v_0 \cdot \{\phi_j\}^T [U(0)] \left\{ \frac{\phi_j}{\sqrt{\mu_z}} \right\}
\end{aligned} \tag{12}$$

When the damping coefficient in Eq. (12) becomes zero or negative, aerodynamic instability occurs, which results in the critical wind speed at 10 m high for aerodynamic instability as

$$v_{0j, cri} = 4 \zeta_j \omega_j M_j^* / \rho \bar{C}_{jF1}^* \tag{13}$$

It can be shown that Eq. (13) will be degenerated to Kolousek's result (1984) if a SDOF system is used with consideration of structural damping, to the Clauert-Hartog criterion (Simiu and Scanlan 1995) if damping is not taken into account, and to Zhang's outcome (1998) if a tower structure is under concern.

3. Derivation of critical wind speed

Since \dot{q}_j (or α) is very small, the third- and higher-order nonlinear terms of \dot{q}_j in Eq. (9) can be neglected without loss of significant influences on galloping analysis. Consequently, Eq. (7) becomes the following explicit nonlinear equation

$$M_j^* \ddot{q}_j(t) + C_j^* \dot{q}_j(t) - C_{jF1}^* \dot{q}_j(t) - C_{jF2}^* \left(\frac{1}{v_0} \right) \dot{q}_j^2(t) + K_j^* q_j(t) = F_j^*(0) \tag{14}$$

To find the critical wind speed $v_{0j, cri}$ with considering the second-order nonlinear term $C_{jF2}^* \dot{q}_j^2$ in Eq. (14), a convenient and efficient way is to solve the following equivalent equation

$$M_j^* \ddot{q}_j(t) + C_j^* \dot{q}_j(t) - \left(C_{jF1}^* + C_{e, jF2}^* \left(\frac{1}{v_0} \right) \right) \dot{q}_j(t) + K_j^* q_j(t) = F_j^*(0) \tag{15}$$

in which equivalent damping coefficient $C_{e, jF2}^*$ can be found with the use of an energy-based equivalent criterion, i.e., energy equally dissipated by the damping terms between equivalent and original systems (i.e., Eqs. (14) and (15)) in each full period. The accuracy of the proposed equivalent approach was verified by Zhang *et al.* (1994) with the use of a Duffing's Oscillator. Applying this equivalent criterion into Eqs. (14) and (15), one can have the following equation

$$\int_0^{2\pi/\omega_j} C_{jF2}^* |\dot{q}_j| \dot{q}_j \cdot \dot{q}_j dt = \int_0^{2\pi/\omega_j} C_{e, jF2}^* \dot{q}_j \cdot \dot{q}_j dt \tag{16}$$

which yields

$$\begin{aligned}
C_{e, jF2}^* &= 8 C_{jF2}^* q_{jm} \omega_j / 3 \pi \\
\bar{C}_{e, jF2}^* &= 8 \bar{C}_{jF2}^* q_{jm} \omega_j / 3 \pi
\end{aligned} \tag{17}$$

where q_{jm} is the maximum value of q_j . The critical wind speed for galloping can then be found from Eq. (15) as

$$C_j^* - C_{jF1}^* - C_{e,jF2}^* \left(\frac{1}{v_0} \right) = 0 \quad (18a)$$

i.e.,

$$2 \zeta_j \omega_j M_j^* - \frac{1}{2} \rho v_0 \bar{C}_{jF1}^* - \frac{1}{2} \rho v_0 \bar{C}_{e,jF2}^* \left(\frac{1}{v_0} \right) = 0 \quad (18b)$$

which results in

$$v_{0j, cri} = 4 \zeta_j \omega_j M_j^* / \rho \left(\bar{C}_{jF1}^* + \bar{C}_{e,jF2}^* \left(\frac{1}{v_{0j, cri}} \right) \right) \quad (18c)$$

or

$$v_{0j, cri} = \frac{4 \zeta_j \omega_j M_j^*}{\rho \bar{C}_{jF1}^*} - \frac{\bar{C}_{e,jF2}^*}{\bar{C}_{jF1}^*} \quad (18d)$$

Eq. (18d) gives an explicit expression for the critical basic wind speed in the j -th mode at height 10 m.

4. Estimation of nonlinear aerodynamic force influences

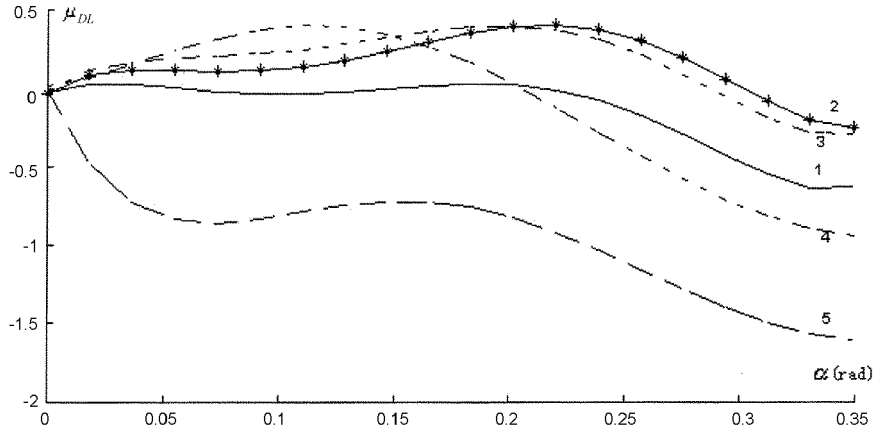
To quantify the influences of nonlinear terms of aerodynamic forces in galloping analysis of MDOF structures, some experimental results for μ_{DL} are selected from Linder (1992), Kajima (1993), Kushioka *et al.* (1996), and Sohankar *et al.* (1997), which are reproduced in Fig. 3. Note there is not enough experimental data for μ_s available for the study.

In the traditional galloping analysis, only the curves with positive slopes at $\alpha=0$ (i.e., curves 1, 2, 3, 4, 6, 7, and 8) will increase the critical wind speed of a structure with cross-sections at almost the same orientation such as towers and bridges.

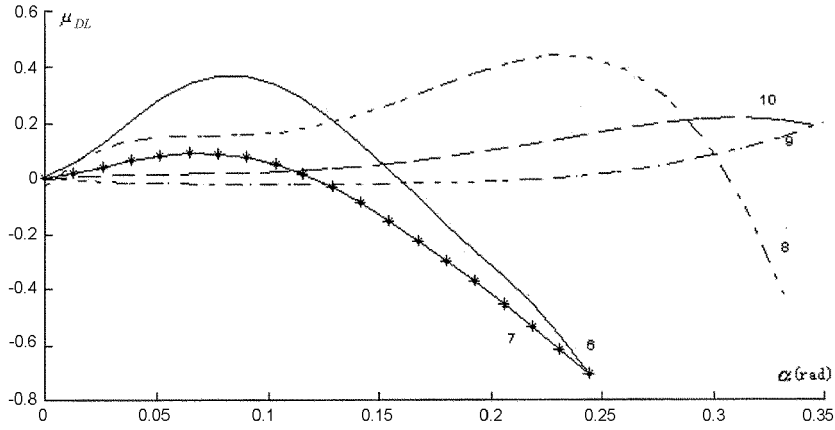
For a structure such as multiple-orientation roof structure, Eq. (18), together with Eqs. (9)-(11) and (17), indicates that the critical wind speed depends on the contributions from each and every sub-area of the structure in which both positive and negative slopes of μ_s or μ_{DL} will have influences in the galloping analysis.

To clearly show the quantitative influences of nonlinear aerodynamic forces in the critical wind speed for galloping phenomena, the following parabolic curves for $\mu(\alpha)$ ($\mu_s(\alpha)$ or $\mu_{DL}(\alpha)$) are assumed on the basis of both the above experimental data and pertinent coefficient characteristics.

$$\begin{aligned} \mu(\alpha) &= a\alpha^2 + b\alpha + c \\ \mu'(\alpha) &= 2a\alpha + b, \mu''(\alpha) = 2a \\ a &= -(\mu_m - c) / \alpha_m^2, b = -2a\alpha_m \end{aligned} \quad (19)$$



(a) 1--K. Kushioka (1996); 2--A. Sohankar (1997); 3--5 A. Okajima (1993)



(b) 6--10 H. Linder (1992)

Fig. 3 Experimental results of curves for $\mu_{DL}-\alpha$ from Linder (1992), Okajima (1993), Kushioka *et al.* (1996), and Sohankar *et al.* (1997)

Substituting Eq. (19) into Eqs. (10) and (17) yields

$$\bar{C}_{jF1}^* = \{\phi_j\}^T [-2a\alpha_m A] \{\phi_j\} \quad (20a)$$

$$\bar{C}_{e,jF2}^* = \{\phi_j\}^T \left[\frac{\mu_z A \cdot 8ay_{jm}\omega_j}{3\pi} \right] \left\{ \left(\frac{\phi_j}{\sqrt{\mu_z}} \right)^2 \right\} \quad (20b)$$

where α_m and y_{jm} are respectively the maximum values of α and d . By neglecting the influence of different vibration modes, the nonlinear influence of the aerodynamic forces on $v_{0j,cri}$ can be quantified by the following ratio η from (18a),

$$\eta = \bar{C}_{e,jF2}^* / \bar{C}_{jF1}^* = -4y_{jm}\omega_j / 3\pi\alpha_m v_{0j,cri} \quad (21a)$$

or directly from (18b)

$$\eta = -\frac{\rho \bar{C}_{e,jF2}^*}{4 \zeta_j \omega_j M_j^*} \quad (21b)$$

Eq. (21a) or (21b) clearly shows that $C_{e,jF2}^*$ is opposite to C_{jF1}^* in sign, resulting in a larger critical wind speed via Eq. (18) by considering the nonlinear terms of aerodynamic forces than the linear terms only. Accordingly, the structure is safer in light of nonlinear influences, which is consistent with those by Novak (1969 and 1972). For illustration, a structure of $H=100$ m is used as an example, in which $\omega_j=6$ rad/sec. Assume that the maximum value of α is $\alpha_m=0.145$. Eq. (18b) then generates the critical basic wind speed $v_{0,cri}=45$ m/s which leads to $y_{im}=0.3$ m. With these data, Eq. (21a) gives the nonlinear influence index η as -12%.

In addition, Eqs. (18) and (21) also reveal that the larger the maximum deformation y_{jm} and natural frequency ω_j of the structure are, the larger the critical wind speed is. Similarly, the larger the value of α_m is, the smaller the critical wind speed is.

5. Applications

The proposed galloping analysis was applied to evaluate the critical wind speed of galloping for the roofs of new Shanghai stadium, which was built in October of 1997 with 80,000 seats and consisting of 32 radial main structures and many secondary structures. As shown in Fig. 4, the shape of the whole roof is approximately an elliptical ring with the longer axes being 288.4 m and 213 m and the shorter axes being 274.4 m and 50 m for the outer and inner ellipse respectively. Each sub-roof has different orientation, making difficult, if not impossible, traditional galloping analysis in comparison with the proposed galloping analysis.

The proposed galloping analysis is used in the roof and results are briefly reported here. A finite-element (FE) model was established for the stadium. Without considering wind direction effects, peak displacements are found to be quite consistent between the data obtained from the FE model and those from pertinent wind-tunnel tests. For instance, the maximum displacement from this



Fig. 4 Side view of new Shanghai stadium, China

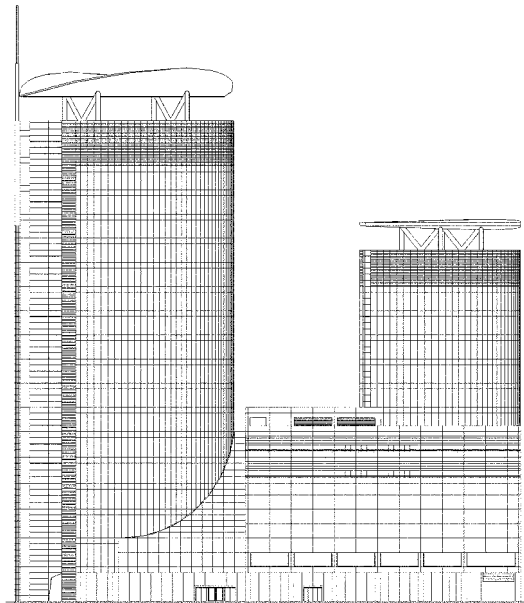


Fig. 5 Roof of a tall building in Suzhou City, Jiangsu Province, China

model approach is 0.176 m, while the corresponding testing data is 0.172 m. The peak stress has a relatively large difference between the model and test. Specifically, the peak stress from the model is 0.873 N/m^2 , while the corresponding test data is 1.193 N/m^2 . The difference of 26.8% is, however, still acceptable from engineering viewpoint. Under the design wind speed 27.44 m/s, neither the FE model with the use of the proposed galloping approach (i.e., use of Eqs. (10) and (13)) nor the wind-tunnel test finds that the galloping will occur. As a matter of fact, immediately after the construction of Shanghai Stadium in August of 1997, a strong typhoon numbered 9711 (wind speed 40 m/s in typhoon center, exceeding the design wind speed) hit Shanghai nearby regions on August 18, 1997. Immediately after that incident, the new Shanghai stadium was examined and no any galloping-related damage was found, implying that the analysis and design based on the proposed method is acceptable.

The proposed galloping analysis was also applied to assess the critical wind speed for the roof of a tall building in Suzhou, China shown in Fig. 5, which is under construction now. For this application, the mean value (i.e., 0.7) of derivatives of ten curves at $\alpha(0)$ in Fig. 3 is used. An FE model was established. The first ten modes were considered in the galloping analysis, in which the fifth to ninth modes are dominant in dynamic responses. Our analysis shows that the lowest critical wind speed is $v_{05.cri}=40.47 \text{ m/s}$, larger than the design wind speed 28.28 m/s. This concludes our analysis that galloping of this roof will not occur.

6. Conclusions

This study extends the traditional SDOF galloping analysis of slender prismatic structures to the MDOF analysis of galloping for roof structures with multiple orientations. In doing so, nonlinear aerodynamic wind forces are considered and an energy-based equivalence technique is used for the

derivation of explicit expression for the critical wind speed of roof galloping. This study confirms that the consideration of the nonlinear aerodynamic forces increases the critical wind speed and thus enhances the aerodynamic stability of structures.

The presented galloping analysis enables an unprecedented understanding of the aerodynamic instability of a broad spectrum of civil structures including the roofs of stadium and building. It can also be conveniently used to aid in efficient design of various structures to resist galloping phenomena.

Further applications of the proposed approach to different structures, together with numerical validation of this study, have been performed and will be reported in the near future.

Acknowledgements

The first author would like to express his appreciation for the financial supports provided by Major Project of National Science Foundation of China, while the second author by the National Science Foundation with Grant Nos. CMS 9896070 and CMS 0085272. The opinions, findings and conclusions expressed herein are those of the authors and do not necessarily reflect the views of the sponsors.

References

- Glauert, H. (1919), "Rotation of an airfoil about a fixed axis", *Aeronautical Research Committee*, R&M 595, Great Britain.
- Hartog, J.P.D. (1932), "Transmission line vibration due to sleet", *Trans. AIEE*, **56**, 1074-1076.
- Hartog, J.P.D. (1956), *Mechanical Vibrations*, McGraw-Hill, New York, N.Y., 4th edition.
- Linder, H. (1992), "Simulation of the turbulence influence on galloping vibrations", *J. Wind Eng. Ind. Aerod.*, **41-44**, 2023-2034.
- Kolousek, V., M. Pirner, O. Fischer and J. Naprstek (1984), *Wind Effects on Civil Engineering Structures*, Elsevier.
- Kushioka, K., T. Ito, A. Honda and K. Hirao (1996), "Prediction by discrete vortex method of aerodynamic forces on smoke stacks of various cross sections", *J. Wind Eng. Ind. Aerod.*, **65**, 309-319.
- Novak, M. (1969), "Aeroelastic galloping of prismatic bodies", *ASCE Journal of Engineering Mechanics Division*, **95**, 115-142.
- Novak, M. (1972), "Galloping oscillations of prismatic structures", *ASCE J. of Engineering Mechanics Division*, **98**, 27-46.
- Okajima, A. (1993), "Numerical study of aeroelastic instability of cylinders with a circular and rectangular cross-section", *J. Wind Eng. Ind. Aerod.*, **46-47**, 541-550.
- Simiu, E. and G. R. Cook (1992), "Empirical fluid elastic models and chaotic galloping: A case study", *J. of Sound & Vibration*, **154**, 45-66.
- Simiu, E. and Scanlan, R.H. (1995), *Wind Effects on Structures-An Introduction to Wind Engineering*, 3th Ed., John Wiley & Sons, New York.
- Sohankar, A., C. Norberg and L. Davidson (1997), "Numerical simulation of unsteady low reynolds number flow around rectangular cylinders at incidence", *J. Wind Eng. Ind. Aerod.*, **69-71**, 189-201.
- Wang, G. and X. Zhang (1998), "Galloping analysis of roof of Shanghai Stadium held 80,000 people", *J. of Structural Engineers*, 82-85 (in Chinese).
- Zhang, X.T. (1998), *The Handbook of Wind-prevented Design and Analysis for Engineering*, China Building Industry Press. (in Chinese).
- Zhang, X.T. Wang Z.P. and Huang B.C. (1994), *Structural Dynamics*, Tongji Univ. Press. (in Chinese).